Dielectric, piezoelectric and electrostrictive properties of antiferroelectric lead-zirconate thin films

Kevin Nadaud, Caroline Borderon, Raphaël Renoud, Micka Bah, Stephane Ginestar, Hartmut Gundel

Journal of Alloys and Compounds 914 (2022) 165340

Contents lists available at ScienceDirect

Journal of Alloys and Compounds

journal homepage: www.elsevier.com/locate/jalcom

Dielectric, piezoelectric and electrostrictive properties of antiferroelectric lead-zirconate thin films

Kevin Nadaud[a,*], Caroline Borderon[b], Raphaël Renoud[b], Micka Bah[a], Stephane Ginestar[b], Hartmut W. Gundel[a]

[a] GREMAN UMR 7347, Université de Tours, CNRS, INSA-CVL, 16 rue Pierre et Marie Curie, Tours 37071, France
[b] IETR, UMR CNRS 6164, Université de Nantes, Nantes 44322, France

ARTICLE INFO

Article history:
Received 19 November 2021
Received in revised form 27 April 2022
Accepted 5 May 2022
Available online 9 May 2022

Keywords:
Antiferroelectric
Electrostrictive effect
Piezoelectric effect

ABSTRACT

Dielectric, piezoelectric and electrostrictive properties of antiferroelectric lead zirconate thin films, elaborated by sol gel on alumina substrates, have been studied as a function of the driving field magnitude E_{AC}. Measurement of the displacement shows that the strain for applied fields below the antiferroelectric-ferroelectric transition is relatively small and that its main contribution arises from the electrostrictive effect. At the same time, due to the presence of a residual ferroelectricity, the piezoelectric effect also contributes to the displacement. At higher fields, a large strain is visible which comes mainly from the antiferroelectric to ferroelectric phase transition, the electrostrictive contribution however still being present. Similar to what has been shown for ferroelectric materials, strain versus the square of polarization loops $S(P^2)$ of the studied antiferroelectric material, exhibit hysteresis character due to the 180° domain walls which contribute to polarization but not to strain. Simultaneous measurement of polarization and displacement enables the extraction of the electrostrictive coefficient and a value $Q = 0.082 \pm 0.009$ m^4 C^{-2} has been obtained. Subtraction of the pure electrostrictive contribution from the displacement curve allows evidencing that the piezoelectric activity coexists with the electrostrictive effect at low fields. Maximum values of the equivalent piezoelectric coefficients are respectively 93 ± 3 pm V^{-1} and 100 ± 3 pm V^{-1} for the positive and the negative parts of the curve for a driving field magnitude $E_{AC} = 700$ kV cm^{-1}.

1. Introduction

Antiferroelectric materials show a double hysteresis loop in the polarization versus electric field characteristics, $P(E)$, presenting interest for energy storage application [1,2]. This family of materials also exhibits large strain, useful for actuators and sensors [2–5]. In this context, materials such as pure or doped $PbZrO_3$ (PZO) have been widely studied [6–9]. For most ferroelectric materials, the electrostrictive contribution is not taken into consideration as the piezoelectric contribution is much larger and predominant [10,11]. In the case of relaxor ferroelectrics, the electrostrictive properties of various materials, including $(1-x)PbMg_{1/3}Nb_{2/3}O_3$-$xPbTiO_3$ (PMN-*x*PT) [12,13], have been studied by measuring the polarization and the displacement simultaneously. In the case of antiferroelectrics, however, the electrostrictive contribution is not negligible at all and needs to be taken into account, especially at low fields [14]. The large strain in antiferroelectric materials comes from the field-induced phase transition to a the ferroelectric phase, and is not due to a purely piezoelectric effect[15,16] since it is visible only above the antiferroeletric to ferroelectric transition field.

In this paper, decorrelation of the different contributions to strain (phase transition, piezoelectric and electrostrictive) is obtained by measuring the dielectric properties and the displacement of a PZO antiferroelectric thin film, as function of the applied electric field for a large range of driving magnitudes below and above the antiferroelectric to ferroelectric transition. Different to what has been reported before for PZO at low fields [14], this enables to access the weight of the electrostrictive contribution to the strain, compared to the piezoelectric and phase transition ones, at each field and allows to extract the electrostrictive coefficient as a function of the driving field magnitude. The simultaneous measurement of the polarization and strain and the use of the strain versus the square of polarization loops $S(P^2)$, permits us to show that 180° domain walls contribute to polarization but not to strain.

* Corresponding author.
E-mail address: kevin.nadaud@univ-tours.fr (K. Nadaud).

https://doi.org/10.1016/j.jallcom.2022.165340
0925-8388/

2. Experiments

The studied PZO antiferroelectric thin films have been elaborated by a sol-gel process onto platinum coated alumina substrates using a multiple spin-coating procedure described elsewhere [7,8]. The studied thin film presents the same crystallographic orientations as in ref. [1], i.e. (100) and (111). Platinum top electrodes of 500 μm × 500 μm have been deposited by sputtering through a shadow mask in order to form a metal-insulator-metal capacitor. Top surface and cross-section images of the thin film have been acquired using scanning electron microscope (Merlin FEG-SEM, Zeiss, Germany).

The electrical and displacement characterizations have been performed with an AixACCT DBLI and TF2000 ferroelectric analyzer (aixACCT Systems GmbH, Germany) using a sine waveform at a frequency of 1 kHz. The polarization and the displacement have been measured simultaneously as a function of the applied AC voltage while increasing the maximum AC voltage from 1 V to 60 V, corresponding to an electric field from 12.5 kV cm^{-1} to 750 kV cm^{-1} applied to the PZO film of 800 nm thickness. In order to improve the signal-to-noise ratio, the results of the $P(E)$ and $S(E)$ loops correspond to the average value of 1000 periods each. Voltage and current waveforms are fitted in order to obtain their phasor representation, $V = |V|e^{j\theta_V}$ and $I = |I|e^{j\theta_I}$ respectively. The computation of the relative permittivity is made using the complex electric impedance $Z = |Z|e^{j\theta_Z}$ of the sample. Its modulus and the angle have been extracted using respectively the ratio and the phase difference, between the applied voltage and the measured current [8]:

$$Z = \frac{V}{I} = \frac{|V|}{|I|}e^{j(\theta_V - \theta_I)} \tag{1}$$

Only the first harmonic of voltage and current are considered for the computation of the modulus and the phase since it is supposed to give the same results than a conventional RLC-meter [17,18]. The real part of the relative permittivity is obtained using the well-known parallel plate capacitor formula:

$$\varepsilon' = \frac{Ct}{S\varepsilon_0} \tag{2}$$

with $\varepsilon_0 = 8.85 \times 10^{-12}$ F m^{-1} the vacuum permittivity, S the area of the electrode and t the thickness of the material. C is the capacitance computed using the complex impedance:

$$C = \mathrm{Re}\left[\frac{1}{j\omega Z}\right] \tag{3}$$

with ω the angular frequency, $2\pi \times 10^3$radians^{-1} in this study and j the imaginary unit.

3. Results and discussion

The top view and cross-section of the elaborated thin film are shown Fig. 1. The film is dense and crack-free. The different layers of the multilayer deposition process, allowing to obtain the desired thickness, are well visible on the cross-section (Fig. 1b).

The polarization as a function of the applied driving electric field of different magnitude values, far below the antiferroelectric-ferroelectric transition field is shown in Fig. 2a. The opening of the $P(E)$ curve can have two origins: (i) large dielectric losses [19,20] or (ii) ferroelectric domain wall pinning/unpinning contributing to the dielectric permittivity [21,22]. In order to discriminate the origin of the opening, the relative permittivity has been computed for each driving field magnitude using the procedure described in the experimental section. The evolution of the relative permittivity with the driving field magnitude is given in Fig. 3. In the 10 kV cm^{-1} to 100 kV cm^{-1} range, the real part of the relative permittivity increases linearly with the driving field magnitude, which corresponds to ferroelectric domain wall pinning/unpinning contribution [8,23,24], since antiferroelectric domain walls cannot move under the effect of a homogeneous field [25]. This residual ferroelectric contribution in antiferroelectric PZO thin films, also called weak ferroelectricity, has already been noticed before by impedance spectroscopy [7,8,14,26]. The weak ferroelectricity is visible on the measured current given in the supplementary material (Figure S1(b)) and corresponds to current peaks at 25 kV cm^{-1} and −89 kV cm^{-1} for increasing and decreasing fields, respectively.

Previous studies show that the ferroelectricity is associated to small clusters, which limits the distance travelled by the domain walls. We thus obtain a relative permittivity lower than predicted by the Rayleigh behavior at medium fields, from 100 kV cm^{-1} to 400 kV cm^{-1}. Above 400 kV cm^{-1}, the permittivity grows faster and goes beyond the Rayleigh law. This comes from the antiferroelectric to ferroelectric phase transition which starts to be visible, implying a large polarization that comes from switching of numerous unit cells[26].

Due to the presence of ferroelectric domain wall motion, the polarization can be modeled in the Rayleigh range using the expression:[24].

$$P = \varepsilon_0\left((\varepsilon_{r-l} + \alpha_r E_{max})E \pm \frac{\alpha}{2}(E_{max}^2 - E^2)\right) \tag{4}$$

with $\varepsilon_{r\text{-}l}$ and α_r respectively the lattice and the domain wall pinning/unpinning contribution. Measurement and modeling ($\varepsilon_{r\text{-}l}$ = 117 and α_r = 0.031 cm kV^{-1}) are compared in the inset of Fig. 2a showing good agreement between both polarization curves. As a consequence, the very small opening of the $P(E)$ loop comes from the ferroelectric domain wall pinning/unpinning contribution and is not due to

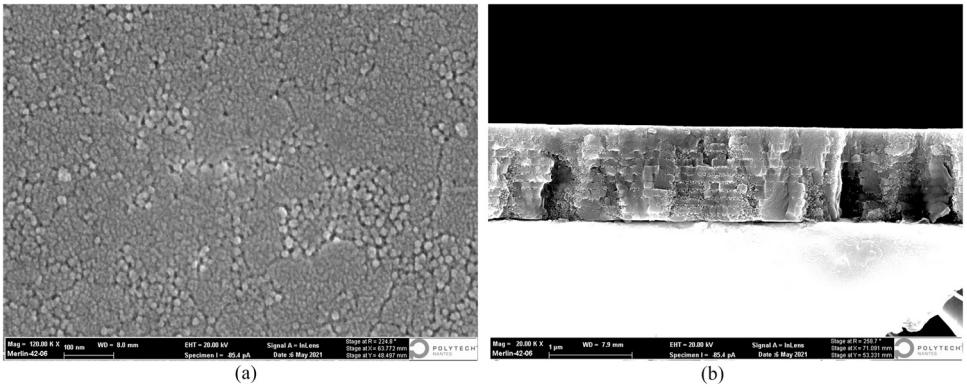

(a) (b)

Fig. 1. Top view (a) and cross section (b) of the elaborated PZO thin film on alumina substrate.

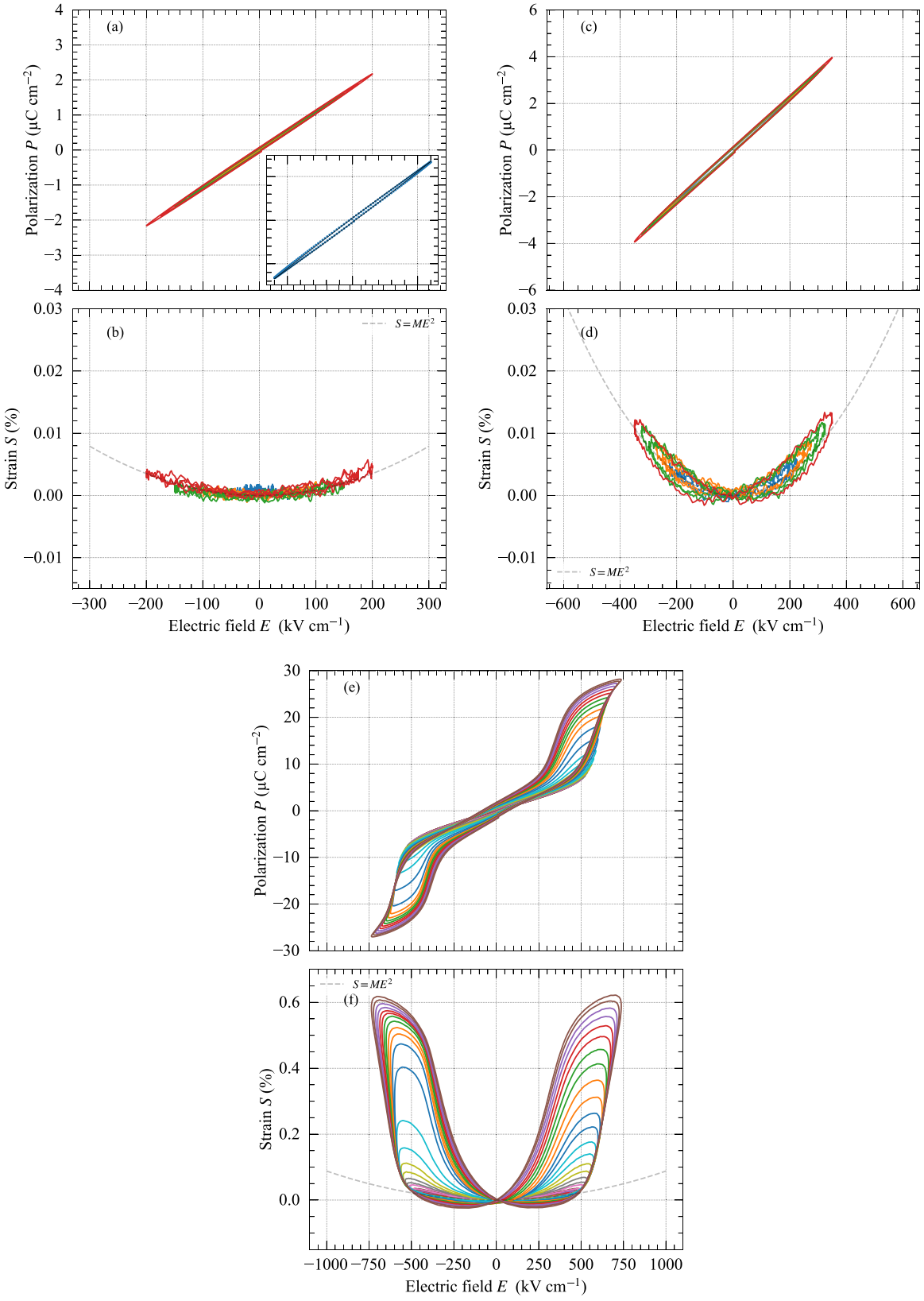

Fig. 2. PZO $P(E)$ loops (a)-(c)-(e) and $S(E)$ loops (b)-(d)-(f) for different values of the maximum magnitude of the driving electric field, from 25 kV cm^{-1} to 200 kV cm^{-1} (a)-(b), from 225 kV cm^{-1} to 350 kV cm^{-1} (c)-(d) and from 375 kV cm^{-1} to 750 kV cm^{-1} (e)-(f). The inset in (a) corresponds to the measured (dot) and modeled (line) polarization for a driving field magnitude of 300 kV cm^{-1}. The dashed line, in (b)-(d)-(f), corresponds to the equation $S = ME^2$ with $M = 8.8 \times 10^{-20}$ C^2 N^{-2}.

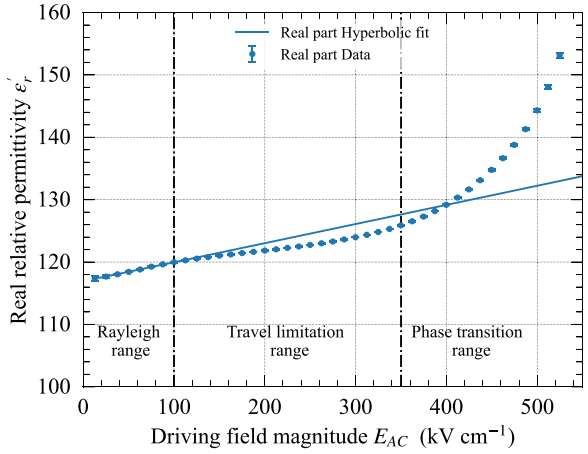

Fig. 3. Real part of the relative permittivity as a function of the driving field magnitude.

dielectric losses, which has already been noticed for $(Pb_{0.97}La_{0.02})(Zr_{0.95}Ti_{0.05})O_3$ (PLZT) thin films [26].

The strain as a function of the electric field, below the antiferroelectric-ferroelectric transition, is reported in Fig. 2b. In the case of a linear dielectric (without ferroelectric contribution) the strain is proportional to the square of the electric field according to the expression:

$$S = ME^2 \quad (5)$$

with M the electric field related electrostrictive coefficient. The quadratic shape of the curves, at low fields, with almost no hysteresis [14], indicates that the main contribution to the strain comes from the electrostrictive effect and not from the piezoelectric effect which should be absent in pure antiferroelectrics due to its centrosymmetry [27]. Almost no deviation from the quadratic behavior (dashed curve in Fig. 2b) is observed. Computing of the electrostrictive coefficient M and fitting of the $S(E)$ curves is presented further below.

The polarization of the PZO as a function of the applied electric field, for medium field magnitudes, is shown in Fig. 2c. Due to the ferroelectric domain wall motion, the hysteresis loop is more open than in the case of the low field measurements. The strain as a function of the applied electric field, for medium fields, is shown in Fig. 2d. Here the hysteresis is well visible and corresponds to a piezoelectric activity caused by the small ferroelectric contribution in the PZO [14], indicating that the strain cannot be described using only the quadratic relation (5).

The polarization of the PZO as a function of the applied electric field, above the antiferroelectric-ferroelectric transition field is shown Fig. 2e. The maximum value of polarization is 28μC/cm^2 which is close to the value reported elsewhere [28]. The antiferroelectric to ferroelectric and the ferroelectric to antiferroelectric transition fields are respectively E_{AF}^{+}= 580 kV cm^{-1} and E_{FA}^{+}= 330 kV cm^{-1} for the positive part and E_{AF}^{-} = −614 kV cm^{-1} and E_{FA}^{-}= − 380 kV cm^{-1} for the negative part of the loops. The strain as a function of the applied electric field above the antiferroelectric-ferroelectric transition, measured for different magnitude values is reported in Fig. 2f. The curve exhibits the butterfly loop characteristic of an antiferroelectric material [14,29] with a maximum strain

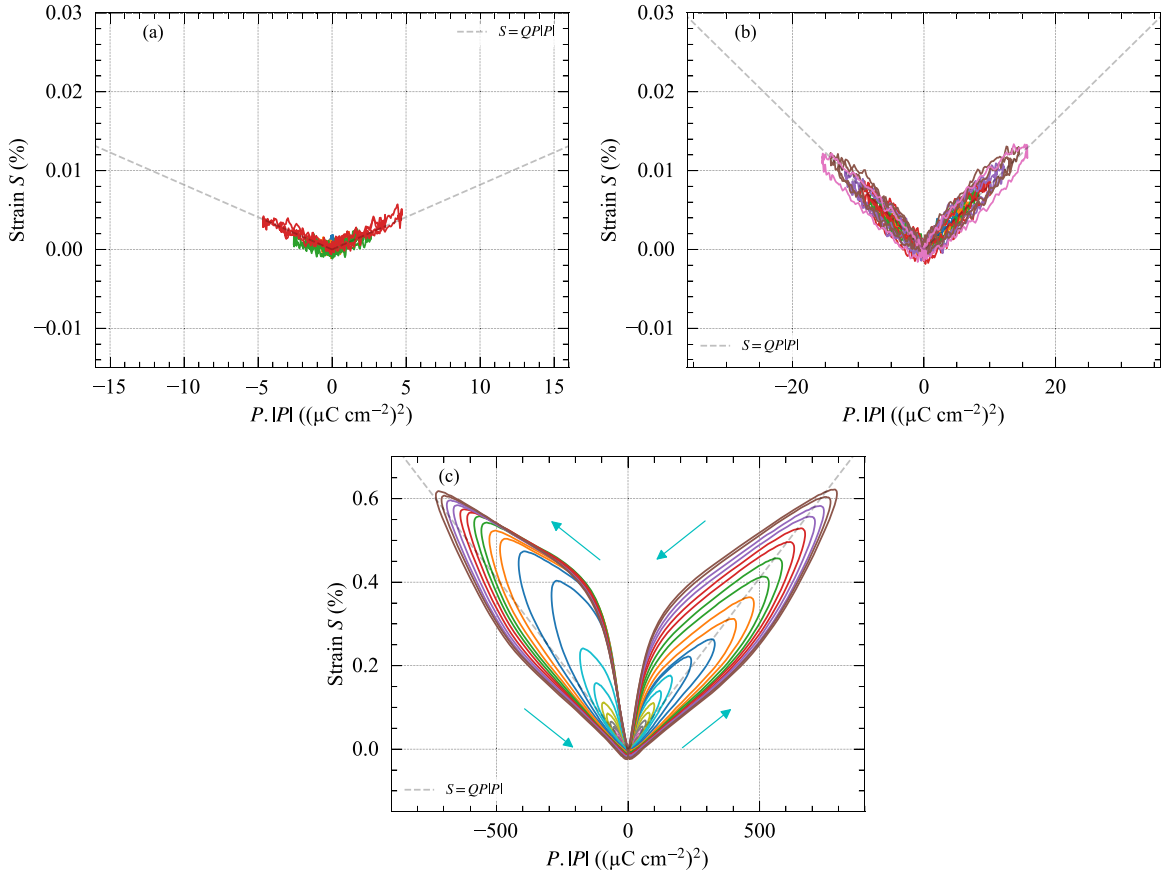

Fig. 4. Strain as a function of the square of polarization for different values of the maximum driving electric field, from 25 kV cm^{-1} to 200 kV cm^{-1} (a), from 225 kV cm^{-1} to 350 kV cm^{-1} (b) and from 375 kV cm^{-1} to 750 kV cm^{-1} (c). For the negative polarization, the square of polarization is taken as negative. The dashed line corresponds to the equation $S = Q_{ave}P|P|$ with Q_{ave} = 0.082 m^4 C^{-2}. Blue arrows on (c) indicate the direction of the hysteresis loop.

of 0.6%, at an electric field of −750 kV cm^{-1}. A slight asymmetry between the positive and the negative side of the loop is visible on the polarization curves (Fig. 2e), especially at the antiferroelectric to ferroelectric transition. The asymmetry in the loops may come from the asymmetry of the sample, i.e. the number of annealing steps for each layer. The first elaborated layer has been annealed twelve times contrary the last one which has been annealed only one time and the layer in between has an intermediate number of annealing. The annealing in air may create oxygen vacancies in the structure which are responsible of imprint and internal bias for ferroelectric material [30,31]. This asymmetry is also visible for PLZT thin films deposited by sol-gel on Pt/Ti/SiO_2/Si substrates [26]. The asymmetry is also visible on the coercive field values of the weak-ferroelectricity contribution (−89 kV cm^{-1} and +25 kV cm^{-1}) and indicates an internal field. The deviation from the quadratic behavior (dashed curve), however, is well visible, indicating that the antiferroelectric-ferroelectric phase transition is at the origin of the large strain. The electrostrictive and piezoelectric contributions, even still present, become the minor contributions at large fields.

In order to estimate the weight of the electrostrictive, piezoelectric and phase transition contribution and to extract the respective coefficients, the electrostrictive strain needs to be subtracted from the measured strain. Hence, the strain has been plotted in Fig. 4 as a function of the square of polarization for different values of the driving field magnitude as suggested by Li *et al* [10,11]. In order to see a possible asymmetry, the square of polarization values are taken negative for negative polarization values [13]. Strain and polarization are linked by the expression: [10,11,14].

$$S = QP^2 \tag{6}$$

with Q the polarization related electrostrictive coefficient. The two electrostrictive coefficients are linked by the expression $M = \varepsilon_0^2 \varepsilon_r^2 Q$ [14]. At low values of the driving field magnitude (Fig. 4a), i.e. below the antiferroelectric-ferroelectric transition, the quadratic relation between strain and polarization is well visible, following the theoretical quadratic law (dashed line). As the driving field magnitude increases, however, still below the antiferroelectric-ferroelectric transition, a hysteresis character in the strain versus driving field curves appears and the quadratic relation is not satisfied anymore (Fig. 2d). This hysteresis has already been reported for ferroelectric materials and may come from the 180° domain walls which contribute to polarization but not to strain [10,11,32]. Even if a hysteresis is visible, the strain versus square of polarization follows the quadratic relation (6) represented by the dashed line (Fig. 4b). At field above the antiferroelectric-ferroelectric transition, the hysteresis is well visible and is attributed to the phase change (Fig. 4c) which contributes less to the strain and to the polarization, similarly to the 180° domain walls.

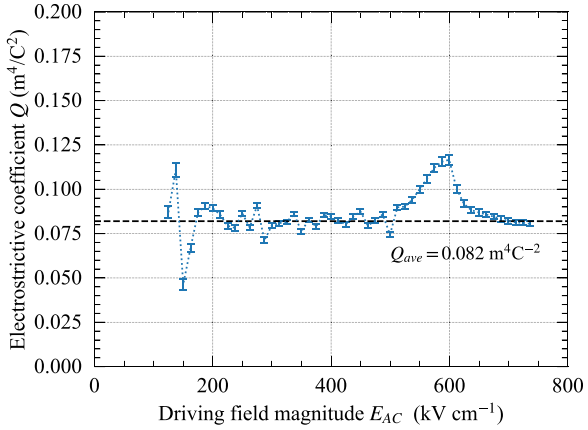

Fig. 5. Electrostrictive coefficient as a function of the driving field magnitude.

Table 1
Electrostrictive coefficient of various material compositions and types.

Material	Type	Q (m^4 C^{-2})	Reference
PMN-0.38PT[a]	Single crystal	0.061	[32]
PMN-0.28PT[a]	Single crystal	0.053	[11]
$PbZrNbO_3$	Single crystal	0.058	[11]
$PbMg_{1/3}Nb_{2/3}O_3$	Single crystal	0.027	[11]
PZT 5 H	Ceramic	0.027[b]	[32]
PZT 4D	Ceramic	0.048[b]	[32]
$BaTiO_3$	Ceramic	0.048[b]	[32]
$PbZrO_3$	Ceramic	0.028	[14]
PLZTS[c]	Ceramic	0.021[b]	[5]
$PbTiO_3$	Thin film	0.05	[33]
$PbZrO_3$	Thin film	0.082 ± 0.009	This work
PMT-0.9PT[a]	Thin film	0.018	[13]
$PbMg_{1/3}Nb_{2/3}O_3$	Thin film	0.0112	[34]
PLZST 65/30/05[d]	Thin film	0.041[b]	[2]
PLZST 75/20/05[d]	Thin film	0.032[b]	[2]
PLZST 90/05/05[d]	Thin film	0.032[b]	[2]
PLZST 85/13/02[d]	Thin film	0.030[b]	[2]

[a] PMN-xPT refers to $(1-x)PbMg_{1/3}Nb_{2/3}O_3$-$xPbTiO_3$.
[b] Value computed using $S(P)$ curves given in the manuscript.
[c] PLZTS refers to $Pb_{0.98}La_{0.02}(Zr_{0.66}Ti_{0.10}Sn_{0.24})_{0.995}O_3$.
[d] PLZST x/y/z refers to $(Pb_{0.97}La_{0.02})(Zr_xSn_yTi_z)O_3$.

Using the $S(P^2)$ curves, the electrostrictive coefficient can be extracted by means of S versus P^2 regression. The obtained values for the different driving field magnitudes are reported Fig. 5. Contrary to the increase of the electrostrictive coefficient Q with growing AC field as noticed by Li *et al* [11], the Q value measured in our case is rather constant up to 500 kV cm^{-1}. At driving fields corresponding to the onset of the antiferroelectric-ferroelectric phase transition (500 kV cm^{-1}), the extracted Q value increases, attains a maximum at the mean transition field (600 kV cm^{-1}), and goes back to its initial value as the material is in the ferroelectric state. This may be due to the hysteresis which disturb the extraction of the electrostrictive coefficient, especially in the phase transition range. The obtained mean value of the electrostrictive coefficient is 0.082 ± 0.009 m^4 C^{-2} which is slightly higher than reported before. This can be attributed to the lower relative permittivity of the studied material, $\varepsilon' = 117$, which is beneficial for a higher electrostrictive coefficient [10]. The electrostrictive coefficients of different materials are summarized in Table 1.

In order to compute the equivalent piezoelectric coefficient, the electrostrictive contribution has been removed from the displacement curve using the electric field related electrostrictive coefficient $M = \varepsilon_0^2 \varepsilon_r^2 Q = 8.8 \times 10^{-20}$ C^2 N^{-2} value, which is close to what is obtained by Dai *et al.* [14]. Here, we use the term "equivalent piezoelectric coefficient" since, for large fields (for example above the antiferroelectric to ferroelectric phase transition), the displacement is mainly due to the phase transition and not to the piezoelectric effect. Nevertheless, the obtained equivalent piezoelectric coefficient permits to compare materials. The calculation has been made using a linear regression from the maximum field value to 0 kV cm^{-1} for positive and negative fields, and for each driving field magnitude. The supplementary material details and illustrates the procedure used for the calculation of the equivalent piezoelectric coefficient which are reported in Fig. 6a.

Below 400 kV cm^{-1}, the positive and negative equivalent piezoelectric coefficients are small but slightly increase with the driving field magnitude due to domain wall pinning/unpinning[21,35]. The coefficients obtained without electrostriction are is very small, indicating almost no piezoelectric activity and that the strain is mainly due to the electrostrictive contribution. With the onset of the antiferroelectric-ferroelectric phase transition (above 550 kV cm^{-1}) a large increase of the equivalent piezoelectric coefficient appears, the value of which saturates when the material is in the ferroelectric phase (above 700 kV cm^{-1}). The coefficients obtained with and

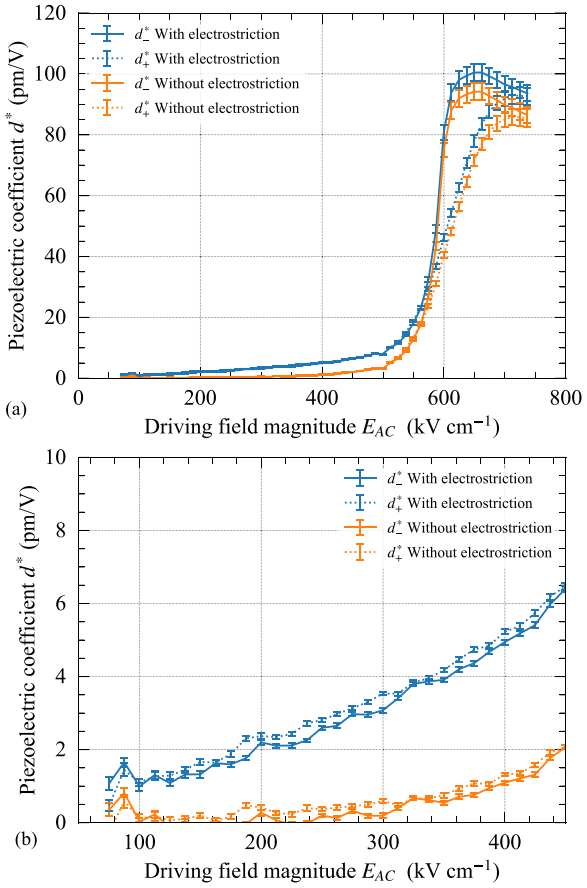

Fig. 6. Equivalent piezoelectric coefficient as a function of the driving field magnitude (a) and magnification of the curves for fields below 450 kV cm^{-1} (b).

without electrostriction are rather similar indicating that the main contribution to the strain comes from the phase transition. The asymmetry noticed on the strain curves (Fig. 2f) is also visible on the equivalent piezoelectric coefficient curves, showing a faster rise for negative driving fields even if the coefficients saturate to almost the same value at the maximum applied field. Without electrostriction, maximum values for the equivalent piezoelectric coefficients are respectively 85 ± 2 pm V^{-1} and 94 ± 3 pm V^{-1} for positive and negative driving field magnitudes of E_{AC} = 750 kV cm^{-1} and E_{AC} = 650 kV cm^{-1}. The coefficients including the electrostrictive contribution are respectively 93 ± 3 pm V^{-1} and 100 ± 3 pm V^{-1} for positive and negative driving fields.

4. Conclusion

In this paper, we study the electrostrictive properties of a PZO antiferroelectric thin film as a function of the driving field magnitude by measuring simultaneously polarization and displacement. We show that the electrostrictive contribution to the strain is predominant at low fields, i.e. at fields below the antiferroelectric-ferroelectric phase transition. In addition to the electrostrictive effect, the piezoelectric effect also contributes to strain at low fields, due to the residual ferroelectricity in the material. At fields corresponding to the antiferroelectric-ferroelectric phase change, the phase-transition contribution becomes the predominant one and a hysteresis behavior is visible on the $S(P^2)$ curves due to 180° domain wall motions which contribute to the polarization but not to the strain.

CRediT authorship contribution statement

Kevin Nadaud: Conceptualization, Methodology, Investigation, Visualization, Writing – original draft. **Caroline Borderon:** Conceptualization, Methodology, Resources, Writing – review & editing. **Raphaël Renoud:** Conceptualization, Methodology. **Micka Bah:** Resources. **Stéphane Ginestar:** Resources. **Hartmut W. Gundel:** Writing – review & editing, Supervision.

Data Availability

The data that support the findings of this study are available from the corresponding author upon reasonable request.

Declaration of Competing Interest

The authors declare that they have no known competing financial interests or personal relationships that could have appeared to influence the work reported in this paper.

Acknowledgments

This work has been performed with the means of the technological platform SMART SENSORS of the French region Pays de la Loire and with the means of the CERTeM (microelectronics technological research and development center) of the French region Centre Val de Loire.

References

[1] M.D. Coulibaly, C. Borderon, R. Renoud, H.W. Gundel, Enhancement of $PbZrO_3$ polarization using a ti seed layer for energy storage application, Thin Solid Films 716 (2020) 138432, https://doi.org/10.1016/j.tsf.2020.138432
[2] M. Sharifzadeh Mirshekarloo, K. Yao, T. Sritharan, Large strain and high energy storage density in orthorhombic perovskite $(Pb_{0.97}La_{0.02})(Zr_{1-x-y}Sn_xTi_y)O_3$, antiferroelectric thin films, Appl. Phys. Lett. 97 (14) (2010) 142902, https://doi.org/10.1063/1.3497193
[3] M. Sharifzadeh Mirshekarloo, L. Zhang, K. Yao, T. Sritharan, Electromechanical properties and fatigue of antiferroelectric (Pb,La)(Zr,Sn,Ti)O_3 thin film cantilevers fabricated by micromachining, Sens. Actuators A: Phys. 187 (2012) 127–131, https://doi.org/10.1016/j.sna.2012.08.024
[4] B. Xu, Y. Ye, L.E. Cross, Dielectric properties and field-induced phase switching of lead zirconate titanate stannate antiferroelectric thick films on silicon substrates, J. Appl. Phys. 87 (5) (2000) 2507–2515, https://doi.org/10.1063/1.372211
[5] S.-E. Park, M.-J. Pan, K. Markowski, S. Yoshikawa, L.E. Cross, Electric field induced phase transition of antiferroelectric lead lanthanum zirconate titanate stannate ceramics, J. Appl. Phys. 82 (4) (1997) 1798–1803, https://doi.org/10.1063/1.365982
[6] K. Yamakawa, S. Trolier-McKinstry, J.P. Dougherty, S.B. Krupanidhi, Reactive magnetron co-sputtered antiferroelectric lead zirconate thin films, Appl. Phys. Lett. 67 (14) (1995) 2014–2016, https://doi.org/10.1063/1.114771
[7] M. Coulibaly, C. Borderon, R. Renoud, H.W. Gundel, Effect of ferroelectric domain walls on the dielectric properties of $PbZrO_3$ thin films, Appl. Phys. Lett. 117 (14) (2020) 142905, https://doi.org/10.1063/5.0017984
[8] K. Nadaud, C. Borderon, R. Renoud, M. Bah, S. Ginestar, H.W. Gundel, Evidence of residual ferroelectric contribution in antiferroelectric lead-zirconate thin films by first-order reversal curves, Appl. Phys. Lett. 118 (4) (2021) 042902, https://doi.org/10.1063/5.0043293
[9] T. Sa, N. Qin, G. Yang, D. Bao, W-doping induced antiferroelectric to ferroelectric phase transition in PbZrO3 thin films prepared by chemical solution deposition, Appl. Phys. Lett. 102 (17) (2013) 172906, https://doi.org/10.1063/1.4803941
[10] F. Li, L. Jin, Z. Xu, S. Zhang, Electrostrictive effect in ferroelectrics: an alternative approach to improve piezoelectricity, Appl. Phys. Rev. 1 (1) (2014) 011103, https://doi.org/10.1063/1.4861260
[11] F. Li, L. Jin, Z. Xu, D. Wang, S. Zhang, Electrostrictive effect in $Pb(Mg_{1/3}Nb_{2/3})O_3$-$xPbTiO_3$ crystals, Appl. Phys. Lett. 102 (15) (2013) 152910, https://doi.org/10.1063/1.4802792
[12] J.-P. Maria, W. Hackenberger, S. Trolier-McKinstry, Phase development and electrical property analysis of pulsed laser deposited $Pb(Mg_{1/3}Nb_{2/3})O_3$-$PbTiO_3$

(70/30) epitaxial thin films, J. Appl. Phys. 84 (9) (1998) 5147–5154, https://doi.org/10.1063/1.368809
[13] Z. Kighelman, D. Damjanovic, N. Setter, Dielectric and electromechanical properties of ferroelectric-relaxor 0.9Pb($Mg_{1/3}Nb_{2/3}$)O_3-0.1 $PbTiO_3$ thin films, J. Appl. Phys. 90 (9) (2001) 4682–4689, https://doi.org/10.1063/1.1409573
[14] X. Dai, J.-F. Li, D. Viehland, Weak ferroelectricity in antiferroelectric lead zirconate, Phys. Rev. B 51 (1995) 2651–2655, https://doi.org/10.1103/PhysRevB.51.2651 ⟨https://link.aps.org/doi/10.1103/PhysRevB.51.2651⟩.
[15] K. Uchino S. Nomura Electro PZT-Fam. antiferroelectrics 50 1 1983 191 196 doi: 10.1080/00150198308014449.
[16] K. Uchino, Antiferroelectric shape Mem. Ceram. 5 (2) (2016) 11, https://doi.org/10.3390/act5020011
[17] I. Fujii, E. Hong, S. Trolier-Mckinstry, Thickness dependence of dielectric nonlinearity of lead zirconate titanate films, ultrasonics, ferroelectrics, and frequency control, IEEE Trans. 57 (8) (2010) 1717–1723, https://doi.org/10.1109/TUFFC.2010.1610
[18] I. Fujii S. Trolier-Mckinstry C. Nies Effect of grain size on dielectric nonlinearity in model BaTiO3 -based multilayer ceramic capacitors 199 28110 2011 194 199 doi: 10.1111/j.1551-2916.2010.04058.x.
[19] G. Catalan, J.F. Scott, Is $CdCr_2S_4$ a multiferroic relaxor? Nature 448 (7156) (2007) E4–E5, https://doi.org/10.1038/nature06156
[20] L. Pintilie, M. Alexe, Ferroelectric-like hysteresis loop in nonferroelectric systems, Appl. Phys. Lett. 87 (11) (2005) 112903, https://doi.org/10.1063/1.2045543
[21] D. Damjanovic, Stress and frequency dependence of the direct piezoelectric effect in ferroelectric ceramics, J. Appl. Phys. 82 (4) (1997) 1788–1797, https://doi.org/10.1063/1.365981
[22] N.B. Gharb, S. Trolier-McKinstry, Dielectric nonlinearity of Pb($Yb_{1/2}$ $Nb_{1/2}$) O_3/$PbTiO_3$ thin films with {100} and {111} crystallographic orientation, J. Appl. Phys. 97 (6) (2005) 064106, https://doi.org/10.1063/1.1857054
[23] C. Borderon, R. Renoud, M. Ragheb, H.W. Gundel, Description of the low field nonlinear dielectric properties of ferroelectric and multiferroic materials, Appl. Phys. Lett. 98 (11) (2011) 112903, https://doi.org/10.1063/1.3567777
[24] D.V. Taylor, D. Damjanovic, Evidence of domain wall contribution to the dielectric permittivity in PZT thin films at sub-switching fields, J. Appl. Phys. 82 (4) (1997) 1973–1975, https://doi.org/10.1063/1.366006
[25] K. Vaideeswaran, K. Shapovalov, P.V. Yudin, A.K. Tagantsev, N. Setter, Moving antiphase boundaries using an external electric field, Appl. Phys. Lett. 107 (19) (2015) 192905, https://doi.org/10.1063/1.4935122
[26] Z. Luo, X. Lou, F. Zhang, Y. Liu, D. Chang, C. Liu, Q. Liu, B. Dkhil, M. Zhang, X. Ren, H. He, Rayleigh-like nonlinear dielectric response and its evolution during electrical fatigue in antiferroelectric (Pb, La)(Zr, Ti) O_3 thin film, Appl. Phys. Lett. 104 (14) (2014) 142904, https://doi.org/10.1063/1.4870992
[27] X. Hao, J. Zhai, L.B. Kong, Z. Xu, A comprehensive review on the progress of lead zirconate-based antiferroelectric materials, Prog. Mater. Sci. 63 (2014) 1–57, https://doi.org/10.1016/j.pmatsci.2014.01.002
[28] P. Ayyub, S. Chattopadhyay, R. Pinto, M.S. Multani, Ferroelectric behavior in thin films of antiferroelectric materials, Phys. Rev. B 57 (1998) R5559–R5562, https://doi.org/10.1103/PhysRevB.57.R5559 ⟨https://link.aps.org/doi/10.1103/PhysRevB.57.R5559⟩.
[29] X. Hao, J. Zhai, F. Shang, J. Zhou, S. An, Orientation-dependent phase switching process and strains of $Pb_{0.97}$ $La_{0.02}$ ($Zr_{0.85}$ $Sn_{0.13}$ $Ti_{0.02}$) O_3 antiferroelectric thin films, J. Appl. Phys. 107 (11) (2010) 116101, https://doi.org/10.1063/1.3407567
[30] G. Le Rhun, R. Bouregba, G. Poullain, Polarization loop deformations of an oxygen deficient Pb($Zr_{0.25}Ti_{0.75}$)O_3 ferroelectric thin film, J. Appl. Phys. 96 (10) (2004) 5712–5721, https://doi.org/10.1063/1.1789635
[31] W. Wu, K.H. Wong, C.L. Choy, Interface-Oxygen-loss-controlled Voltage Offsets in Epitaxial Pb(Zr0.52Ti0.48)O3 thin-film capacitors with La0.7Sr0.3MnO3 electrodes, Applied Physics Letters, American Institute of Physics,, 2004, pp. 5013–5015, https://doi.org/10.1063/1.1827929 http://aip.scitation.org/doi/10.1063/1.1827929.
[32] G. Viola, T. Saunders, X. Wei, K.B. Chong, H. Luo, M.J. Reece, H. Yan, Contribution of piezoelectric effect, electrostriction and ferroelectric/ferroelastic switching to strain-electric field response of dielectrics, J. Adv. Dielectr. 03 (01) (2013) 1350007, https://doi.org/10.1142/s2010135×13500070
[33] Z. Kighelman, D. Damjanovic, M. Cantoni, N. Setter, Properties of ferroelectric $PbTiO_3$ thin films, J. Appl. Phys. 91 (3) (2002) 1495–1501, https://doi.org/10.1063/1.1431432
[34] Z. Kighelman, D. Damjanovic, N. Setter, Electromechanical properties and self-polarization in relaxor Pb($Mg_{1/3}Nb_{2/3}$)O_3 thin films, J. Appl. Phys. 89 (2) (2001) 1393–1401, https://doi.org/10.1063/1.1331339
[35] D.V. Taylor, D. Damjanovic, Piezoelectric properties of rhombohedral Pb(Zr,Ti)O_3 thin films with (100), (111), and “random” crystallographic orientation, Appl. Phys. Lett. 76 (12) (2000) 1615–1617, https://doi.org/10.1063/1.126113